Acta Crystallographica Section D
Biological Crystallography
ISSN 0907-4449

Isothiazolidinone (IZD) as a phosphoryl mimetic in inhibitors of the *Yersinia pestis* protein tyrosine phosphatase YopH

Sung-Eun Kim,[a] Medhanit Bahta,[a] George T. Lountos,[b] Robert G. Ulrich,[c] Terrence R. Burke Jr[a]* and David S. Waugh[b]*

[a]Chemical Biology Laboratory, National Cancer Institute at Frederick, PO Box B, Frederick, MD 21702-1201, USA, [b]Macromolecular Crystallography Laboratory, National Cancer Institute at Frederick, PO Box B, Frederick, MD 21702-1201, USA, and [c]Laboratory of Molecular Immunology, United States Army Medical Research Institute of Infectious Diseases, Frederick, MD 21702, USA

Correspondence e-mail: tburke@helix.nih.gov, waughd@mail.nih.gov

Received 11 April 2011
Accepted 16 May 2011

PDB Reference: YopH–3-(1,1-dioxido-3-oxoisothiazolidin-5-yl)benzaldehyde complex, 2ydu.

Isothiazolidinone (IZD) heterocycles can act as effective components of protein tyrosine phosphatase (PTP) inhibitors by simultaneously replicating the binding interactions of both a phosphoryl group and a highly conserved water molecule, as exemplified by the structures of several PTP1B–inhibitor complexes. In the first unambiguous demonstration of IZD interactions with a PTP other than PTP1B, it is shown by X-ray crystallography that the IZD motif binds within the catalytic site of the *Yersinia pestis* PTP YopH by similarly displacing a highly conserved water molecule. It is also shown that IZD-based bidentate ligands can inhibit YopH in a nonpromiscuous fashion at low micromolar concentrations. Hence, the IZD moiety may represent a useful starting point for the development of YopH inhibitors.

1. Introduction

Yersinia pestis, a member of the Gram-negative Enterobacteriaceae family, has played an important role in human history as the causative agent of plague. For pathogenicity, *Y. pestis* relies on several essential virulence factors, including the protein tyrosine phosphatase (PTP) YopH (Zhang *et al.*, 1992). Accordingly, inhibitors of YopH may be of value in the event of a bioterrorist attack with *Y. pestis*.

Catalysis by YopH involves the transfer of the substrate arylphosphoryl group to the thiolate anion of Cys403, which is part of the PTP signature motif (P-loop) Cys-Xxx-Ala-Gly-Xxx-Gly-Arg (residues 403–409). In general, the defining nature of substrate interaction with the P-loop has made the inclusion of anionic arylphosphoryl mimicking functionality a critical feature of PTP inhibitor design (Zhang, 2002; Tautz & Mustelin, 2007; Shen *et al.*, 2010; Combs, 2010). Recently, it has been reported that isothiazolidinone (IZD) heterocycles can serve as particularly effective phosphoryl mimetics in PTP1B inhibitors (Combs *et al.*, 2006; Yue *et al.*, 2006; Ala, Gonneville, Hillman, Becker-Pasha, Wei *et al.*, 2006; Sparks *et al.*, 2007; Douty *et al.*, 2008). The key to the high PTP1B-binding affinity of IZD motifs is their combined ability to replicate the binding interactions of the phosphoryl group and to replace a highly conserved water molecule found in the catalytic sites of many PTP1B cocrystal structures (Ala, Gonneville, Hillman, Becker-Pasha, Wei *et al.*, 2005; Combs, 2007). The current study was undertaken to determine whether similar mimicry could be applied in the case of YopH.

2. Materials and methods

2.1. Synthetic organic chemistry

2.1.1. 2-(*tert*-Butyl)-5-chloroisothiazol-3(2*H*)-one 1,1-dioxide (1). Compound **1** was synthesized as described by Lewis *et al.* (1971*a*,*b*).

2.1.2. 2-(*tert*-Butyl)-5-[3-(hydroxymethyl)phenyl]isothiazol-3(2*H*)-one 1,1-dioxide (2). To a solution of **1** (1.01 g, 4.5 mmol) in 1,4-dioxane (100 ml) was added 3-(hydroxymethyl)phenylboronic acid (1.03 g, 6.8 mmol), [1,1′-bis(diphenylphosphino)ferrocene]dichloropalladium(II) complex with dichloromethane (1:1) (0.74 g, 0.9 mmol) and K_2CO_3 (3.13 g, 22.6 mmol) and the mixture was stirred and heated under reflux (8 h). The mixture was filtered through Celite and the Celite was washed with 30 ml dichloromethane (CH_2Cl_2) and 30 ml ethyl acetate (EtOAc). The combined organic layer was evaporated *in vacuo* and purified by silica-gel chromatography to yield **2** as a pale yellow solid product (1.17 g, 88% yield). ESI-MS (*m*/*z*): calculated for $C_{14}H_{17}NO_4S$, 295.09; found, 318.0 $(M + Na)^+$.

2.1.3. 2-(*tert*-Butyl)-5-[3-(hydroxymethyl)phenyl]isothiazolidin-3-one 1,1-dioxide (3). To a solution of **2** (1.02 g, 3.5 mmol) in 20 ml tetrahydrofuran (THF) at 273 K was added 2 *M* lithium borohydride ($LiBH_4$) in THF (1.9 ml, 3.8 mmol) dropwise over 10 min and the reaction mixture was stirred at 273 K (20 min). The reaction was quenched by the addition of 10 ml saturated aqueous ammonium chloride (NH_4Cl), partioned between EtOAc (20 ml) and H_2O (20 ml) and then dried with magnesium sulfate ($MgSO_4$), filtered and organic solvent removed. Purification by silica-gel chromatography provided **3** as an off-white solid product (0.89 g, 87% yield). ESI-MS (*m*/*z*): calculated for $C_{14}H_{19}NO_4S$, 297.1; found, 320.2 $(M + Na)^+$.

2.1.4. 3-[2-(*tert*-Butyl)-1,1-dioxido-3-oxoisothiazolidin-5-yl]benzaldehyde (4). To a solution of **3** (0.15 g, 0.5 mmol) in CH_2Cl_2 (20 ml) at 273 K was added Dess–Martin periodinane [1,1,1-triacetoxy-1,1-dihydro-1,2-benziodoxol-3(1*H*)-one; Dess & Martin, 1983] (0.26 g, 0.6 mmol) and the mixture was stirred at 273 K (2 h). The solvent was removed *in vacuo*, the residue was partitioned between EtOAc (10 ml) and H_2O (10 ml) and the organic layer was washed with brine (10 ml), dried ($MgSO_4$) and organic solvent removed. Purification by silica-gel chromatography provided **4** as an off-white solid product (0.15 g, 96% yield). ESI-MS (*m*/*z*): calculated for $C_{14}H_{17}NO_4S$, 295.09; found, 296.1 $(M + H)^+$.

2.1.5. 3-(1,1-Dioxido-3-oxoisothiazolidin-5-yl)benzaldehyde (5). A solution of **4** (0.1 g, 0.34 mmol) in TFA (2 ml) was irradiated in a microwave reactor (413 K, 1 min). The mixture was concentrated *in vacuo* and the residue was purified by preparative HPLC [Waters Prep-LC 4000 system with a Phenomenex Gemini 10 µm C_{18} 110 Å column (250 × 21.20 mm) at a flow rate of 10 ml min^{-1} with a mobile phase of *A* = 0.1% aqueous TFA and *B* = 0.1% TFA in aqueous acetonitrile with UV monitoring at 220, 254 and 280 nm] to afford **5** as an off-white solid product (0.017 g, 21% yield). ESI-MS (*m*/*z*): calculated for $C_{10}H_9NO_4S$, 239.03; found, 238.0 $(M - H)^-$.

2.1.6. 3-(1,1-Dioxido-3-oxoisothiazolidin-5-yl)benzaldehyde *O*-[3-(aminooxy)propyl] oxime (6). To a solution of **5** (0.05 g, 0.21 mmol) and *O*,*O*′-1,3-propanediylbishydroxylamine hydrochloride (0.224 g, 1.25 mmol) in 3 ml dimethylsulfoxide (DMSO) was added 30 µl acetic acid (AcOH). The reaction mixture was agitated at 273 K (overnight). The reaction mixture was purified directly by HPLC to provide **6** as a white solid product (0.08 g, 90% yield). ESI-MS (*m*/*z*): calculated for $C_{13}H_{17}N_3O_5S$, 327.09; found, 326.0 $(M - H)^-$.

2.1.7. General procedure for the synthesis of heterobidentate products (7a–7i). A mixture of **6** (15 µl of a 24 m*M* solution in DMSO), the appropriate aldehyde (**a**–**i**) (15 µl of a 24 m*M* solution in DMSO) and AcOH (15 µl of a 48 m*M* solution in DMSO) were gently agitated at 273 K (overnight) to provide oxime products (45 µl at 8 m*M* in DMSO). Purity analysis by HPLC showed that the reactions afforded the desired oxime products (**7a**–**7i**) in greater than 90% yield. Crude reaction mixtures were used directly for biological evaluation.

2.1.8. 3-(4-Methylfuran-2-yl)-1-phenyl-1*H*-pyrazole-4-carbaldehyde *O*-[3-({[3-(1,1-dioxido-3-oxoisothiazolidin-5-yl)benzylidene]amino}oxy)propyl] oxime (7h). To a solution of **6** (5 mg, 0.011 mmol) and 3-(4-methylfuran-2-yl)-1-phenyl-1*H*-pyrazole-4-carbaldehyde (3.14 mg, 0.012 mmol) in DMSO (0.3 ml) was added 5 µl AcOH and the mixture was agitated at 273 K (overnight). The reaction mixture was subjected to direct purification by HPLC to provide **7h** as a white solid (2.6 mg, 41% yield). ESI-MS (*m*/*z*): calculated for $C_{28}H_{27}N_5O_6S$, 561.16; found, 562.1 $(M + H)^-$, 584.1 $(M + Na)^+$. HRMS-ESI (*m*/*z*): calculated for $C_{28}H_{27}N_5O_6S$, 561.17; found, 562.18 $(M + H)^-$.

2.2. Determination of IC_{50} values of YopH inhibitors

The following reagents used in YopH enzyme assays were obtained from Sigma–Aldrich: *para*-nitrophenyl phosphate (*p*NPP) tablets, 30% bovine serum albumin (BSA) solution (protease-free), 1.0 *M* HEPES solution pH 7.0–7.6 and dithiothreitol (DTT). Aqueous ethylenediaminetetraacetic acid, sodium salt (EDTA; 0.5 *M*, pH 8.0) was obtained from Invitrogen and 96-well plates were purchased from Costar. Optical densities were measured with a Biotek Synergy 2 spectrophotometer at A_{abs} 405 nm using absolute readout for determination of IC_{50} values. The catalytic domain of YopH (residues 164–468) was expressed in *Escherichia coli* and purified as described previously (Zhang *et al.*, 1992; Phan *et al.*, 2003). Total reaction volumes of 100 µl per well were used in 96-well plates. Buffer was prepared by mixing 25 m*M* HEPES buffer pH 7.0–7.6, 50 m*M* NaCl, 2.5 m*M* EDTA and 5 m*M* DTT, with 1 m*M* fresh DTT added immediately prior to the start of the assays. To each well was added 79 µl assay buffer, 5 µl 0.25% BSA followed by 5 µl of inhibitors in DMSO at dilutions of 400, 133, 44, 15, 5, 1.67, 0.56, 0.19, 0.063, 0.032 and 0 µ*M*. To the reaction mixture was then added 5 µl of YopH in buffer (25 µg ml^{-1}) followed by 6 µl 10 m*M* *p*NPP buffer and each plate was agitated gently at 298 K for 15–20 min. Hydrolysis of the substrate was immediately measured from

Table 1
X-ray diffraction data-collection and refinement statistics.

Values in parentheses are for the highest resolution shell.

X-ray source	MicroMax-007 HF
Wavelength (Å)	1.5418
Resolution (Å)	50–1.79 (1.84–1.79)
Space group	$P2_12_12_1$
Unit-cell parameters	
a (Å)	49.3
b (Å)	55.9
c (Å)	99.1
Total reflections	165007 (5712)
Unique reflections	25845 (1680)
Completeness (%)	95.7 (63.4)
$R_{\rm merge}$† (%)	5.4 (40.9)
$\langle I/\sigma(I)\rangle$	35.5 (2.6)
Multiplicity	6.4 (3.4)
Refinement statistics	
Resolution (Å)	50–1.79
No. of reflections (working set/test set)	24486/1302 (1236/63)
$R_{\rm work}$‡ (%)	17.8 (36.5)
$R_{\rm free}$‡ (%)	21.3 (43.6)
No. of atoms	
Protein	2186
Inhibitor	16
Water	276
Mean *B* factors (Å^2)	
Protein	27.4
Inhibitor	34.3
Water	35.9
R.m.s. deviations from ideal geometry	
Bond lengths (Å)	0.015
Bond angles (°)	1.6
Ramachandran plot	
Most favored (%)	91.6
Additionally allowed (%)	7.6
Generously allowed (%)	0.8
Disallowed (%)	0
PDB code	2ydu

† $R_{\rm merge} = \sum_{hkl}\sum_i |I_i(hkl) - \langle I(hkl)\rangle|/\sum_{hkl}\sum_i I_i(hkl)$, where $\langle I(hkl)\rangle$ is the mean intensity of multiply recorded reflections. ‡ $R = \sum_{hkl}||F_{\rm obs}| - |F_{\rm calc}||/\sum_{hkl}|F_{\rm obs}|$. $R_{\rm free}$ is the *R* value calculated for 5% of the data set that was not included in the refinement.

optical densities at $A_{\rm abs}$ 405 nm. IC_{50} values were determined by fitting the data to sigmoidal curves generated using the Boltzmann equation.

2.3. X-ray crystallography

The PTPase domain of YopH (residues 164–468) was expressed in *E. coli* and purified as described previously (Zhang *et al.*, 1992; Phan *et al.*, 2003). The purified protein was pooled and concentrated by diafiltration to 17.6 mg ml^{-1} in 100 m*M* sodium acetate pH 5.7, 100 m*M* NaCl and 1 m*M* EDTA. Crystals of YopH were obtained using condition E8 [0.1 *M* buffer system 2 pH 7.5, 0.12 *M* ethylene glycol, 12.5%(*v*/*v*) MPD, 12.5%(*w*/*v*) PEG 1000 and 12.5%(*w*/*v*) PEG 3350] of the Morpheus Screen (Gorrec, 2009) from Molecular Dimensions (Apopka, Florida, USA). A 1:1 ratio of protein solution (17.6 mg ml^{-1}) to well solution was used for crystallization at 293 K. Plate-like crystals grew within 3 d. To obtain the protein–inhibitor complex, compound **5** was dissolved in DMSO and added to the crystallization solution to obtain a final concentration of 5 m*M* (10% DMSO). The crystals were added to the soaking solution and soaked for 48 h at room temperature. Crystals were flash-frozen in liquid nitrogen without the need for an additional cryoprotectant.

X-ray diffraction data for the YopH–compound **5** complex were collected at 100 K from a single crystal using a MAR345 detector mounted on a Rigaku MicroMax-007 HF high-intensity microfocus rotating-anode X-ray generator with VariMax HF optics (Rigaku Corporation, The Woodlands, Texas, USA) operated at 40 kV and 30 mA. 180 frames of data were collected using an exposure time of 5 min, an oscillation angle of 1° and a crystal-to-detector distance of 120 mm. The X-ray diffraction data were processed with *HKL*-3000 (Minor *et al.*, 2006). Data-collection and refinement statistics are outlined in Table 1. The structure was solved by molecular replacement using the *MOLREP* program (Vagin & Teplyakov, 2010) from the *CCP*4 suite (Winn *et al.*, 2011) and the coordinates of the previously solved YopH structure (PDB code 1qz0) after removing all solvent and ligand atoms (Phan *et al.*, 2003). Cross-rotation and translation searches were performed using data to 3.0 Å resolution followed by rigid-body refinement with *REFMAC*5 (Murshudov *et al.*, 2011). Iterative rounds of model rebuilding and refinement were performed with *Coot* (Emsley & Cowtan, 2004) and *REFMAC*5 and the location of the inhibitor was unambiguously identified using $\sigma_{\rm A}$-weighted $2mF_{\rm o} - DF_{\rm c}$ and $mF_{\rm o} - DF_{\rm c}$ electron-density maps (Read, 1997). The coordinates and refinement restraint files were prepared using the Dundee *PRODRG* server (Schüttelkopf & van Aalten, 2004). Water molecules were located using *Coot* and were refined with *REFMAC*5. The refinement was monitored by setting aside 5% of the reflections for calculation of the $R_{\rm free}$ value (Brünger, 1993). Model validation was performed using *MolProbity* (Chen *et al.*, 2010). The coordinates and structure-factor files were deposited in the Protein Data Bank with accession code 2ydu.

3. Results and discussion

3.1. Identification of a key conserved water within the catalytic cavity of YopH

In order to identify whether a similarly conserved water molecule exists in the catalytic binding site of YopH, we employed our previously reported cocrystal structure of the peptide Asp-Ala-Asp-Glu-F_2Pmp-Leu bound to YopH (PDB entry 1qz0; Phan *et al.*, 2003), where F_2Pmp represents the nonhydrolyzable pTyr mimetic phosphonodifluoromethyl phenylalanine (Burke *et al.*, 1993, 1994), along with YopH cocrystal structures containing PO_4^{3-} (PDB entry 1lyv; A. G. Evdokimov, D. S. Waugh, K. Routzahn, J. Tropea & S. Cherry, unpublished work), SO_3^{2-} (PDB entry 1yts; Schubert *et al.*, 1995), WO_4^{2-} (PBD entry 1ytw; Fauman *et al.*, 1996) and HVO_4^{2-} (PBD entry 2i42; J. Vijayalakshmi & M. A. Saper, unpublished work). Superposition of these structures onto 1qz0 revealed the presence of a single co-localized water molecule, identified as WC (red), Wa4 (magenta), Wa23 (cyan), Wa20 (yellow) and Wa12 (blue) in the respective structures (Fig. 1*a*). Furthermore, superposition onto 1qz0 of

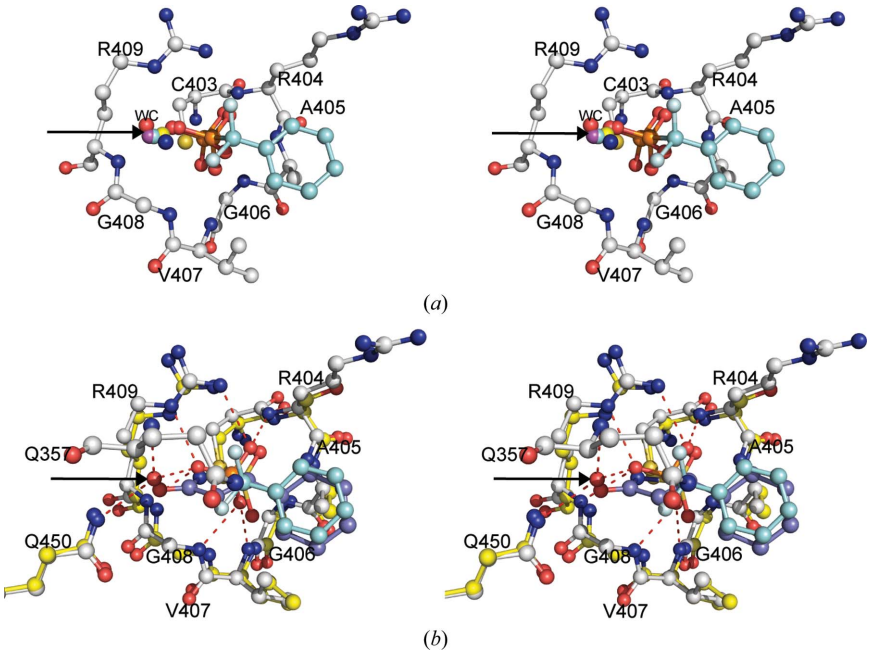

Figure 1
Analysis of PDB crystal structure data. (*a*) YopH signature motif (residues 403–409; PDB entry 1qz0) with conserved water molecules shown color-coded to match PDB entries (red, 1qz0; magenta, 2i42; cyan, 1lyv; yellow, 1yts; blue, 1ytw). Also shown are bound phosphonodifluoromethylphenyl (cyan; PDB entry 1qz0) and phosphate (PDB entry 1lyv) groups. (*b*) YopH catalytic site hydrogen-bonding network involving a phosphonodifluoromethylphenyl group (cyan) and conserved water (WC; PDB entry 1qz0) superimposed with the catalytic motif of PTP1B (yellow) and its bound (*S*)-IZD phenyl group (slate; PBD entry 2cm7). Of note is the coincidence of the IZD carbonyl O atom with the conserved YopH water molecule, which is highlighted by an arrow.

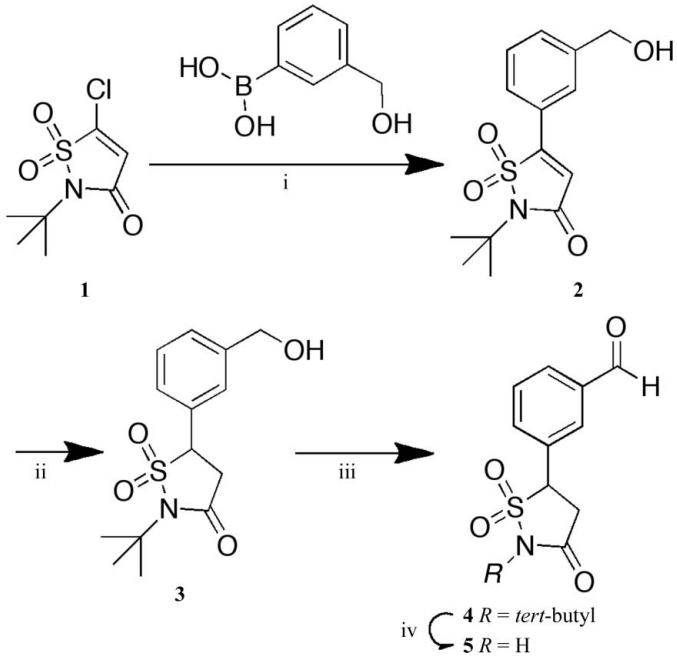

Figure 2
Synthesis of IZD-containing fragment **5**. (i) [1,1′-bis(diphenylphosphino)ferrocene]palladium(II) dichloride–CH_2Cl_2, K_2CO_3, 1,4-dioxane, reflux (88% yield); (ii) $LiBH_4$, THF, 273 K (87% yield); (iii) Dess–Martin periodinane, 273 K (96% yield); (iv) TFA, 413 K (microwave, 1 min) (21% yield).

an IZD-containing PTP1B cocrystal structure (PBD entry 2cm7; Ala, Gonneville, Hillman, Becker-Pasha, Yue *et al.*, 2006) showed that the identified conserved WC water in 1qz0 is coincident with the IZD carbonyl O atom of the PTP1B structure. It was also noted that the N and both O atoms of the IZD sulfonimide group showed good overlap with the three O atoms of the difluoromethylphosphonic acid (DFMP) group (Fig. 1*b*). This suggested that recognition of IZD by YopH and PTP1B could occur in a similar fashion.

3.2. Synthesis of IZD-containing compound 5

In order to determine if and how an IZD group might bind within the catalytic cleft of YopH, we prepared 3-(1,1-dioxido-3-oxoisothiazolidin-5-yl)benzaldehyde (**5**), which contained a 3-formyl group on the aryl ring that would allow subsequent elaboration *via* oxime ligation (Fig. 2; Liu *et al.*, 2010). The synthesis of **5** employed Suzuki coupling of the known chloroheterocycle **1** (Yue *et al.*, 2006) with commercially available 3-(hydroxymethyl)phenylboronic acid to yield the 3-hydroxymethyl-containing **2**. Reduction of the heterocycle double bond ($LiBH_4$ in THF; Combs, Yue, Bower, Zhu *et al.*, 2005) provided the racemic saturated congener **3**, which was subjected to oxidation of the benzylic alcohol using Dess–Martin periodinane conditions (Dess & Martin, 1983) to yield the corresponding aldehyde (**4**). Hydrolysis of the *tert*-butyl group using neat TFA under microwave irradiation gave the desired IZD construct **5**. It should be noted that the isomeric variant of **5** with the formyl group at the phenyl 4-position appears in the patent literature, although its synthesis is not given (Combs, Yue, Bower, Zhu *et al.*, 2005).

3.3. X-ray cocrystal structure of YopH in complex with IZD-containing compound 5

We solved the cocrystal structure of **5** in complex with YopH, thus providing the first opportunity to observe IZD-binding interactions in a phosphatase other than PTP1B [PDB entries corresponding to PTP1B–IZD complexes include 2veu, 2vew, 2vev, 2vex and 2vey (Douty *et al.*, 2008), 2cm2, 2cm3, 2cm7, 2cm8, 2cma, 2cmb and 2cmc (Ala, Gonneville, Hillman, Becker-Pasha, Yue *et al.*, 2006) and 2cne, 2cnf, 2cng, 2cnh and 2cni (Ala, Gonneville, Hillman, Becker-Pasha, Wei *et al.*, 2006)]. It has previously been reported that cocrystallization of PTP1B with diastereomeric ligands bearing unresolved (*R*/*S*)-IZD groups resulted in selective binding of the (*S*)-IZD forms (for examples, see PBD entries 2cm7, 2cma, 2cng, 2cnh and 2cni). This was consistent with the fact that the potencies of PTP1B inhibitors bearing (*S*)-IZD groups are significantly

greater than those of the corresponding (*R*)-IZD-containing isomers (Combs, Yue, Bower, Ala *et al.*, 2005; Ala, Gonneville, Hillman, Becker-Pasha, Wei *et al.*, 2006; Ala, Gonneville, Hillman, Becker-Pasha, Yue *et al.*, 2006). While our cocrystal structure of YopH in complex with compound **5** (Fig. 2) also employed a racemic ligand, structural refinement of the electron density for YopH-bound **5** using (*S*)-restraints and (*R*)-restraints for **5** could not unambiguously distinguish a preference for one IZD chirality over the other (Figs. 3*a* and 3*b*). Indeed, superimposing the ligand structures obtained using (*S*)-restraints and (*R*)-restraints showed remarkably good overlap (Fig. 3*c*). These observations are consistent with the previous finding that in PTP1B cocrystal structures with both (*S*)-IZD and its achiral unsaturated homologue the aryl ring and IZD heteroatoms occupy the same positions (Ala, Gonneville, Hillman, Becker-Pasha, Yue *et al.*, 2006; Yue *et al.*, 2006). We subjected the two cocrystal structures bearing (*S*)-**5** and (*R*)-**5** to energy minimization using a flexible ligand/rigid protein model (*ICM Pro* software v.3.7-2af/MacOSX; http://www.molsoft.com; Abagyan *et al.*, 2009) and found that the calculated binding scores for both (*S*)- and (*R*)-enantiomers were highly similar. Given the near-indistinguishable nature of complexes based on the (*S*)- and (*R*)-enantiomers, subsequent modeling employed the (*S*)-enantiomer of **5** .

The YopH–**5** cocrystal structure reveals that the interactions of **5** within the catalytic pocket consist of six hydrogen bonds, two arising from each of the three IZD O atoms. Specifically, two hydrogen bonds exist between one IZD sulfonamide O atom and the guanidinium group of Arg409 and the amide proton of Arg404, two hydrogen bonds originate from the second sulfonamide oxygen to the amide protons of Gly406 and Val407, and the IZD carbonyl O atom forms hydrogen bonds to the Asp356 amide and the side-chain carboxamide of Gln450 (Fig. 4*a*). These combined interactions replicate those observed with the DFMP group in the 1qz0 structure, with the exception that the IZD carbonyl O atom replaces and mimics the catalytically conserved water (WC) in the original YopH-bound DFMP structure (Fig. 4*b*).

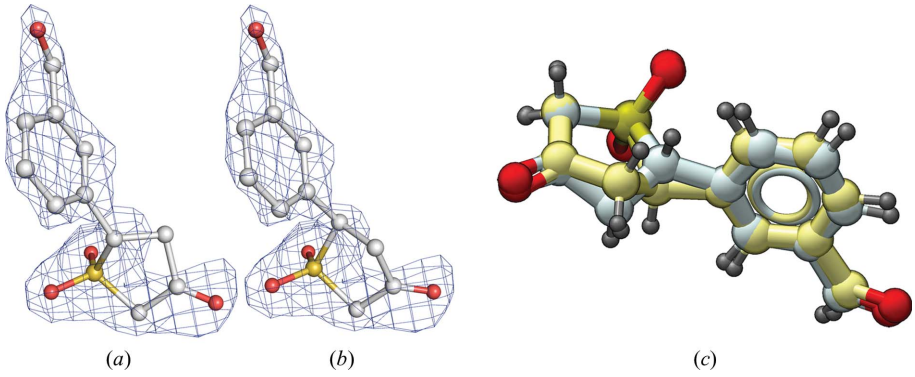

Figure 3
Comparison of YopH-bound **5** refined using (*S*)–(*R*) chirality. Overlay of the $2mF_o - DF_c$ electron-density maps (1.79 Å resolution, contoured at the 1σ level) of YopH-bound **5** onto ligands refined using (*a*) (*S*)-restraints and (*b*) (*R*)-restraints. (*c*) Superposition of the structures: (*S*)-**5**, C atoms in white; (*R*)-**5**, C atoms in yellow.

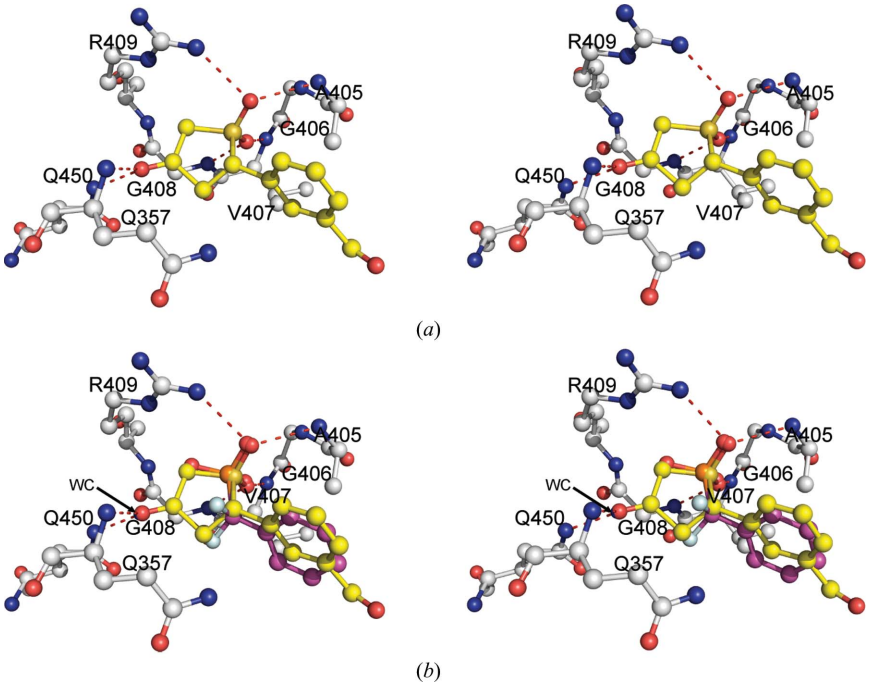

Figure 4
Crystal structure of YopH-bound **5**. (*a*) Hydrogen-bonding interactions (shown as red dashes) of **5** (yellow) with catalytic site residues. (*b*) Superposition onto (*a*) of PDB entry 1qz0 showing the relative alignment of the phosphonodifluoromethylphenyl group (magenta) and the catalytically conserved WC water (shown in blue). In both (*a*) and (*b*), ligand **5** is shown in the (*S*)-configuration.

3.4. Utilization of compound 5 for the synthesis of bidentate inhibitors

While the IZD motif affords good interactions within the catalytic pocket, the effective recognition of substrates by PTPs involves both binding of the phenylphosphoryl group within the catalytic cleft and interactions of secondary elements with proximal regions of the protein. Accordingly, one approach to the design of PTP inhibitors is to use bidentate constructs containing at least one phenylphosphate mimetic (Chen & Seto, 2002, 2004; Xie & Seto, 2005, 2007; Srinivasan *et al.*, 2006, 2008; Yu *et al.*, 2007; Tan *et al.*, 2009). We have previously reported tethered bidentate YopH inhibitors that were formed from aldehyde-containing fragments using oxime bond-forming bis-aminooxy-containing linkers (Liu *et al.*, 2010). Our earlier work employed a 5-formyl-2-hydroxybenzoic acid frag-

Table 2
IC_{50} values of YopH inhibitors.

Inhibitor	IC_{50} (μM)
7a	78
7b	18
7c	13
7d	12
7e	11
7f	5
7g	4
7h	2
7i	2

ment as the phenylphosphate-mimicking portion. Others have also shown the utility of this motif in the design of bidentate YopH inhibitors (Tautz *et al.*, 2005; Leone *et al.*, 2010; Huang *et al.*, 2010). In the current study, the IZD-containing fragment **5** served as the phenylphosphoryl replacement. Reaction of **5** with an excess of *O*,*O*′-1,3-propanediylbishydroxylamine hydrochloride in DMSO with AcOH gave the corresponding mono-oxime **7** in 90% HPLC-purified yield (Fig. 5). Further reaction of **7** with structurally diverse aldehydes yielded the corresponding heterobidentate constructs (**7a**–**7i**). An advantage of oxime ligation is that the reaction-product mixtures can be biologically evaluated without purification. The compounds **7a**–**7i** were evaluated using a colorimetric assay that measured their ability to inhibit the YopH-mediated hydrolysis of *p*-nitrophenylphosphate (Liu *et al.*, 2010). Inhibitory potencies (IC_{50} values) varied 40-fold, ranging from 78 μM for **7a** to 2 μM for **7h** and **7i** (Table 2).

The development of PTP inhibitors is often accompanied by a high incidence of false positives that arise from nonspecific mechanisms (McGovern *et al.*, 2002, 2003; Feng *et al.*, 2005). In order to determine whether promiscuous mechanisms were involved in inhibition by the most potent compounds (**7h** and **7i**), YopH assays were conducted in the presence and absence of 0.01% TX-100, since it is known that promiscuous inhibition can often be minimized by the addition of such a detergent (Ryan *et al.*, 2003). While the potency of **7h** was unchanged in the presence of detergent, the IC_{50} value of **7i** was dramatically shifted from its original value of 2 μM to >100 μM in the presence of detergent (data not shown). This data suggests that **7i** could be acting through promiscuous mechanisms.

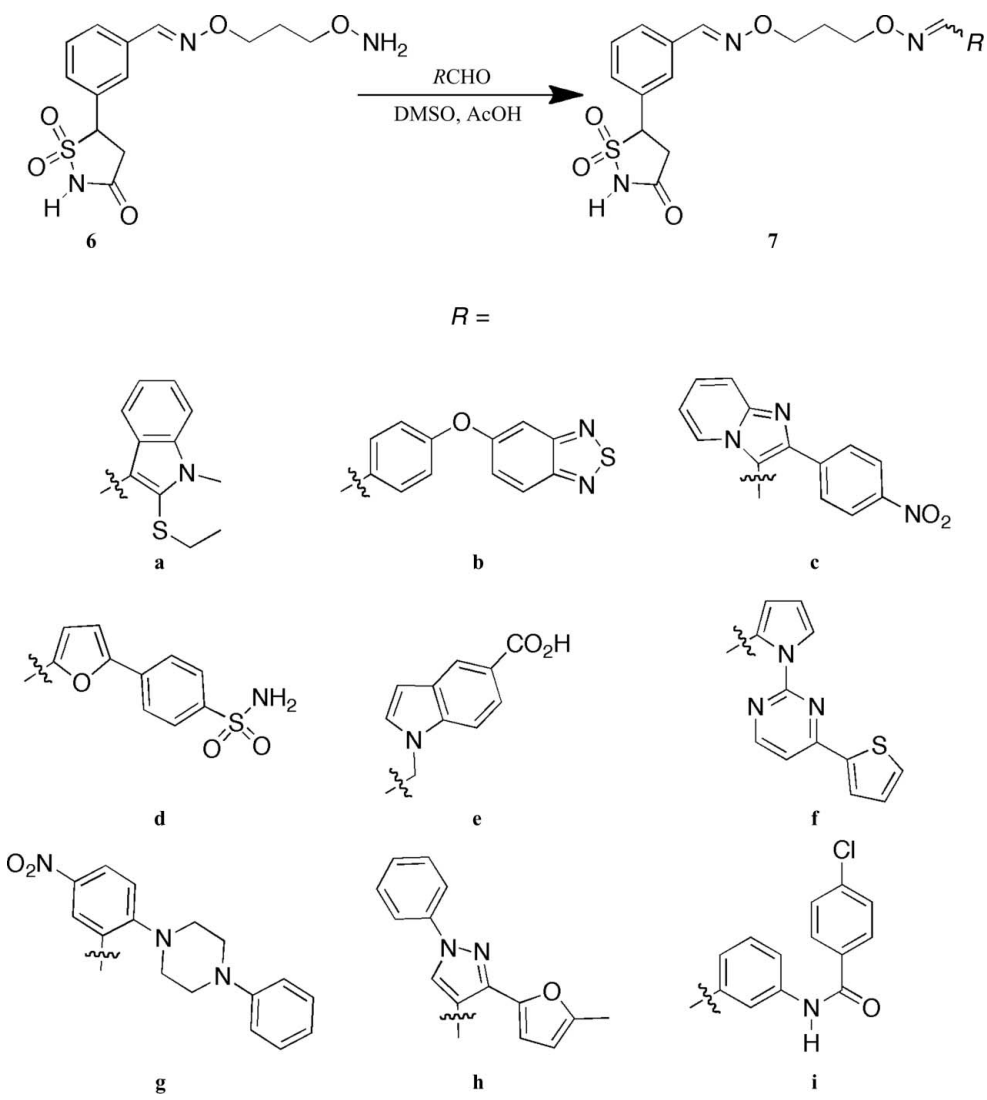

Figure 5
Synthesis of bidentate YopH inhibitors.

4. Conclusions

In summary, our current YopH–**5** cocrystal structure provides the first demonstration of IZD-binding interactions in a phosphatase other than PTP1B. This structure shows that the IZD carbonyl O atom mimics a highly conserved water molecule in a fashion similar to that observed in PTP1B. In addition, there is good correspondence of the IZD sulfonimide group with the phosphonic acid O atoms of a YopH-bound high-affinity DFPM group. Using the IZD-containing **5** as an anchor, we were able to prepare heterobidentate ligands with low-micromolar affinity. Taken together, these results provide potentially useful insights into the design of YopH inhibitors.

Appreciation is expressed to Afroz Sultana (LMI) for technical support and to Joseph Tropea and Scott Cherry (MCL) for purification of YopH. Elec-

trospray mass-spectrometry experiments were conducted on the LC/ESMS instrument maintained by the Biophysics Resource in the Structural Biophysics Laboratory, Center for Cancer Research, National Cancer Institute at Frederick. This work was supported in part by the Intramural Research Program of the NIH, Center for Cancer Research, NCI-Frederick and the National Cancer Institute, National Institutes of Health and the Joint Science and Technology Office of the Department of Defense. The content of this publication does not necessarily reflect the views or policies of the Department of Health and Human Services, nor does mention of trade names, commercial products, or organizations imply endorsement by the US Government.

References

Abagyan, R. A., Orry, A., Raush, E., Budagyan, L. & Totrov, M. (2009). *ICM Manual* 3.0. MolSoft LLC, La Jolla, California, USA.
Ala, P. J., Gonneville, L., Hillman, M., Becker-Pasha, M., Wei, M. *et al.* (2006). *J. Biol. Chem.* **281**, 32784–32795.
Ala, P. J., Gonneville, L., Hillman, M., Becker-Pasha, M., Yue, E. W. *et al.* (2006). *J. Biol. Chem.* **281**, 38013–38021.
Brünger, A. T. (1993). *Acta Cryst.* D**49**, 24–36.
Burke, T. R., Kole, H. K. & Roller, P. P. (1994). *Biochem. Biophys. Res. Commun.* **204**, 129–134.
Burke, T. R., Smyth, M. S., Nomizu, M., Otaka, A. & Roller, P. P. (1993). *J. Org. Chem.* **58**, 1336–1340.
Chen, Y. T. & Seto, C. T. (2002). *J. Med. Chem.* **45**, 3946–3952.
Chen, Y. T. & Seto, C. T. (2004). *Bioorg. Med. Chem.* **12**, 3289–3298.
Combs, A. P. (2007). *IDrugs*, **10**, 112–115.
Combs, A. P. (2010). *J. Med. Chem.* **53**, 2333–2344.
Combs, A. P. *et al.* (2006). *J. Med. Chem.* **49**, 3774–3789.
Combs, A. P., Yue, E. W., Bower, M., Ala, P. J. *et al.* (2005). *J. Med. Chem.* **48**, 6544–6548.
Combs, A. P., Yue, E. W., Bower, M. J., Zhu, W., Crawley, M. L., Sparks, R. B., Pruitt, J. R. & Takvorian, A. (2005). US Patent 7141596.
Chen, V. B., Arendall, W. B., Headd, J. J., Keedy, D. A., Immormino, R. M., Kapral, G. J., Murray, L. W., Richardson, J. S. & Richardson, D. C. (2010). *Acta Cryst.* D**66**, 12–21.
Dess, D. B. & Martin, J. C. (1983). *J. Org. Chem.* **48**, 4155–4156.
Douty, B., Wayland, B., Ala, P. J., Bower, M. J., Pruitt, J., Bostrom, L., Wei, M., Klabe, R., Gonneville, L., Wynn, R., Burn, T. C., Liu, P. C., Combs, A. P. & Yue, E. W. (2008). *Bioorg. Med. Chem. Lett.* **18**, 66–71.
Emsley, P. & Cowtan, K. (2004). *Acta Cryst.* D**60**, 2126–2132.
Fauman, E. B., Yuvaniyama, C., Schubert, H. L., Stuckey, J. A. & Saper, M. A. (1996). *J. Biol. Chem.* **271**, 18780–18788.
Feng, B. Y., Shelat, A., Doman, T. N., Guy, R. K. & Shoichet, B. K. (2005). *Nature Chem. Biol.* **1**, 146–148.
Gorrec, F. (2009). *J. Appl. Cryst.* **42**, 1035–1042.
Huang, Z., He, Y., Zhang, X., Gunawan, A., Wu, L., Zhang, Z. Y. & Wong, C. F. (2010). *Chem. Biol. Drug Des.* **76**, 85–99.
Leone, M., Barile, E., Vazquez, J., Mei, A., Guiney, D., Dahl, R. & Pellecchia, M. (2010). *Chem. Biol. Drug Des.* **76**, 10–16.
Lewis, S. N., Miller, G. A., Hausman, M. & Szamborski, E. C. (1971*a*). *J. Heterocycl. Chem.* **8**, 571–580.
Lewis, S. N., Miller, G. A., Hausman, M. & Szamborski, E. C. (1971*b*). *J. Heterocycl. Chem.* **8**, 591–595.
Liu, F., Hakami, R. M., Dyas, B., Bahta, M., Lountos, G. T., Waugh, D. S., Ulrich, R. G. & Burke, T. R. Jr (2010). *Bioorg. Med. Chem. Lett.* **20**, 2813–2816.
McGovern, S. L., Caselli, E., Grigorieff, N. & Shoichet, B. K. (2002). *J. Med. Chem.* **45**, 1712–1722.
McGovern, S. L., Helfand, B. T., Feng, B. & Shoichet, B. K. (2003). *J. Med. Chem.* **46**, 4265–4272.
Minor, W., Cymborowski, M., Otwinowski, Z. & Chruszcz, M. (2006). *Acta Cryst.* D**62**, 859–866.
Murshudov, G. N., Skubák, P., Lebedev, A. A., Pannu, N. S., Steiner, R. A., Nicholls, R. A., Winn, M. D., Long, F. & Vagin, A. A. (2011). *Acta Cryst.* D**67**, 355–367.
Phan, J., Lee, K., Cherry, S., Tropea, J. E., Burke, T. R. & Waugh, D. S. (2003). *Biochemistry*, **42**, 13113–13121.
Read, R. J. (1997). *Methods Enzymol.* **277**, 110–128.
Ryan, A. J., Gray, N. M., Lowe, P. N. & Chung, C. (2003). *J. Med. Chem.* **46**, 3448–3451.
Schubert, H. L., Fauman, E. B., Stuckey, J. A., Dixon, J. E. & Saper, M. A. (1995). *Protein Sci.* **4**, 1904–1913.
Schüttelkopf, A. W. & van Aalten, D. M. F. (2004). *Acta Cryst.* D**60**, 1355–1363.
Shen, K., Qi, L. & Stiff, L. (2010). *Curr. Pharm. Des.* **16**, 3101–3117.
Sparks, R. B., Polam, P., Zhu, W., Crawley, M. L., Takvorian, A., McLaughlin, E., Wei, M., Ala, P. J., Gonneville, L., Taylor, N., Li, Y., Wynn, R., Burn, T. C., Liu, P. C. & Combs, A. P. (2007). *Bioorg. Med. Chem. Lett.* **17**, 736–740.
Srinivasan, R., Tan, L. P., Wu, H. & Yao, S. Q. (2008). *Org. Lett.* **10**, 2295–2298.
Srinivasan, R., Uttamchandani, M. & Yao, S. Q. (2006). *Org. Lett.* **8**, 713–716.
Tan, L. P., Wu, H., Yang, P.-Y., Kalesh, K. A., Zhang, X., Hu, M., Srinivasan, R. & Yao, S. Q. (2009). *Org. Lett.* **11**, 5102–5105.
Tautz, L., Bruckner, S., Sareth, S., Alonso, A., Bogetz, J., Bottini, N., Pellecchia, M. & Mustelin, T. (2005). *J. Biol. Chem.* **280**, 9400–9408.
Tautz, L. & Mustelin, T. (2007). *Methods*, **42**, 250–260.
Vagin, A. & Teplyakov, A. (2010). *Acta Cryst.* D**66**, 22–25.
Winn, M. D. *et al.* (2011). *Acta Cryst.* D**67**, 235–242.
Xie, J. & Seto, C. T. (2005). *Bioorg. Med. Chem.* **13**, 2981–2991.
Xie, J. & Seto, C. T. (2007). *Bioorg. Med. Chem.* **15**, 458–473.
Yu, X., Sun, J.-P., He, Y., Guo, X., Liu, S., Zhou, B., Hudmon, A. & Zhang, Z.-Y. (2007). *Proc. Natl Acad. Sci. USA*. **104**, 19767–19772.
Yue, E. W. *et al.* (2006). *Bioorg. Med. Chem.* **14**, 5833–5849.
Zhang, Z.-Y. (2002). *Annu. Rev. Pharmacol. Toxicol.* **42**, 209–234.
Zhang, Z.-Y., Clemens, J. C., Schubert, H. L., Stuckey, J. A., Fischer, M. W., Hume, D. M., Saper, M. A. & Dixon, J. E. (1992). *J. Biol. Chem.* **267**, 23759–23766.